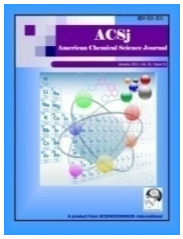

American Chemical Science Journal
3(3): 264-286, 2013

SCIENCEDOMAIN *international*
www.sciencedomain.org

Characterization Studies of Aluminum Alloy Substrate Surfaces Treated By Oxyanion Esters of A-Hydroxy Acids and Their Salts

Volkan Cicek[1*]

[1]*Department of Educational Management, Ishik University, Erbil, Iraq.*

Author's contribution

The only author performed the whole research work. Author VC designed the study, performed the statistical analysis, wrote the protocol, wrote the first draft of the manuscript, managed the analyses of the study, and the literature searches. Author VC read and approved the final manuscript.

Research Article

Received 18th March 2013
Accepted 3rd May 2013
Published 24th May 2013

ABSTRACT

In this investigation, first, substrate coupons of commonly used alloys of Aluminum, which are 2024, 6061 and 7075 alloys, were immersed in solutions of inhibitors such as gluconate esters having the formula of (M)x(hydroxyacid)y(M'aOb)z combining constituents that are already known for high inhibition efficiencies such as hydroxyacids and metal oxyanions. Among other inhibitor solutions used were benzilate esters, gluconate salts, zinc carboxylates, etc. Secondly, after immersions of the mild steel coupons in inhibitors solutions of varying concentrations for different periods of time, they were characterized by means of various surface techniques such as FT-IR, X-Ray, SEM, XPS and digital imaging. As a result of use of these characterization techniques, it is decided whether protective layers of inhibitor compounds are formed on the substrate surfaces due to immersions in the solutions of the inhibitor compounds similar to those of conversion coatings. The results have proven individual consequences for each inhibitor tried and are described in detail herein the paper, which assisted in the assessment of aqueous corrosion inhibition mechanisms of mild steel by oxyanion esters of α-hydroxy acids and their salts.

**Corresponding author: Email: volkancicek@gmail.com;*

Keywords: Conversion coating; inhibition efficiency; immersion; oxyanion; photoelectron; weight-loss.

1. INTRODUCTION

Corrosion inhibitors that were used for immersions of aluminum alloy coupons were synthesized via a single precursor method described in detail in author's previous studies that are available in the literature [1-5]. Common characteristics of these inhibitors are that they are environmentally friendly metallo-organic corrosion inhibitors for protection of mild steel and certain aluminum alloys aimed to replace hexavalent chromium based corrosion inhibitors. For this reason, several corrosion inhibiting species such as hydroxyacids and metal oxyanions were combined in a single compound with the general formula, $(M)_x(\text{hydroxyacid})_y(M'_aO_b)_z$. These were tested alongside the individual components in order to determine whether there were any synergistic interactions. It is also important to note that most of the chosen individual components were corrosion inhibitors that were previously commercialized. Some of these species such as gluconates were commercially available resulting in their direct use with no synthesis required. The common commercial use for these readily available gluconates is in the field of medicinal health as nutritional supplements. Such gluconates of zinc, calcium, magnesium and sodium were used and tested throughout this study as corrosion inhibitors, precursors, or constituents of synergistic corrosion inhibitor formulations.

2. MATERIALS AND METHODS

2.1 Preparation of Substrate Coupons of Aluminum Alloys

Coupons are described as small pieces of metal, usually of rectangular shape, which are inserted in the process stream and removed after a period of time that is greater than 24 hours. For the preparation of coupons, commercially available aluminum alloy metal sheets of sufficient thickness were cut in dimensions of 1x1 inch as seen in Fig. 1. A hole is drilled at the corner of the coupon so that the coupon could be hanged in solution via a durable polymeric material such as a fishing-line that does not corrode.

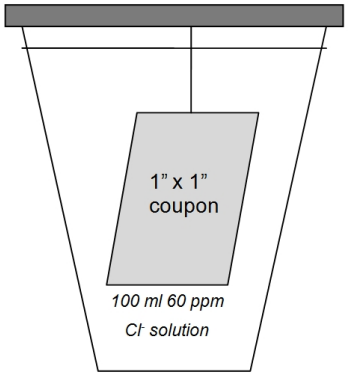

Fig. 1. Immersion apparatus

Standards determined for Preparing Specimens for Weight-Loss Tests by ASTM (American Society for Testing and Materials) were followed with no alteration [6-7]. For mild steel

specimens, the first step is described as degreasing in an organic solvent or hot alkaline cleaner or both. Aluminum alloy specimens used in this study were cut out of large rolls of aluminum alloy sheets that were previously greased for corrosion prevention. This grease was removed from the aluminum alloy coupons by dipping them in hexane and rubbing them with paper towels soaked with hexane when necessary. Secondly, coupons were placed in Oakite Products Inc. brand Oakite-164 alkaline cleaner solution at 150ºF for 10 minutes to complete degreasing of the coupons. Lastly, pickling of the aluminum alloy coupons is performed to remove the remaining oxides or tarnish.

Oakite solution was prepared by dissolving 60 g of Oakite detergent in 1000 ml of water at 180ºF. After degreasing and cleaning, the coupons were weighed and fully immersed in 100 ml solutions of 60 ppm Cl^- and various concentrations of inhibitors for various periods of time (3 days, 7 days or for 14 days). As a controlled variable, 100 ml has been chosen as the volume of the solution due to the low amount of inhibitors that was required. Another controlled variable was the salt content of the solution, which was chosen as 60 ppm Cl^- since it is a situation commonly encountered in cooling water systems based on mild steel construction [8].

Immersion periods of 3, 7 and 14 day periods were chosen since periods less than 24 hours are not enough for the system to come into an equilibrium, while a period of more than 14 days was too long to test many samples, that are needed for comparison purposes [9]. Given that accelerated corrosion is required, a period of 7 days has been determined to be the optimum period of immersion at room temperature.

2.2 Qualitative Analysis of the Coupons after Immersions

Visual inspection of the coupons compared to the control coupons after completion of immersions but before removal of corrosion products has been a useful qualitative method. When the images of coupons treated with molybdenum esters of ydroxyl-acids and those of controls are compared, it is found that coupons treated with molybdate esters had a nonuniform black colored deposition along with depositions of corrosion products around a few pits. The black color is indicative of the presence of molybdenum oxide and hydroxides in a mixed Mo(V)/Mo(VI) oxidation state.

2.2.1 Aluminum 2024 alloy

Among the images shown in Fig. 2, apart from the control coupon that had deposition of corrosion products, the potassium benzilate molybdate treated coupon revealed black colored depositions similar to the ones reported in the literature. For instance, thin colored films of molybdenum oxides produced by molybdate salts on Al 7075-T6 alloy that provide slight corrosion resistance have been reported in the literature [10].

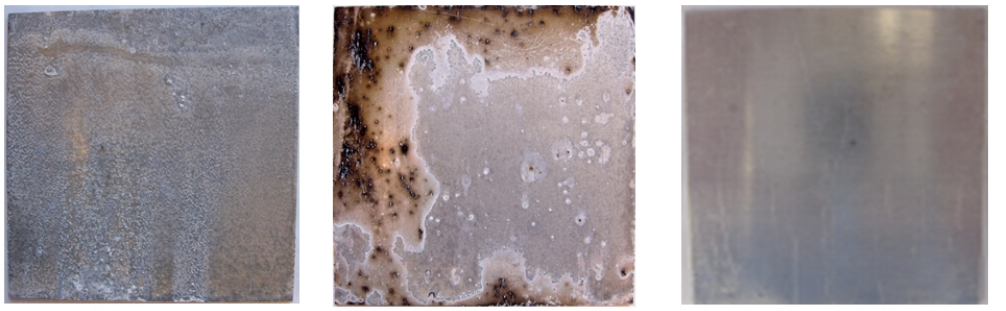

Al 2024 alloy control in 0.5M Cl- soln. for 1 week

200 ppm K(benzilate)molybdate in 0.5 M Cl- soln. for 1 week

200 ppm Zn(gluconate)vanadate in 0.5M Cl- soln. for 1 week

Fig. 2. Images of Al 2024 Alloy Control Coupon and Sample Coupons Immersed in Solutions of Metal Oxyanion Esters; Respectively

Many other studies have also reported black-colored molybdate coatings on various metal surfaces [11-15]. On the other hand; coupons treated with inhibitors that resulted in high inhibition efficiencies had visually clear surfaces. Among these are zinc gluconate vanadate, potassium benzilate vanadate, and chromium oxyhydroxide. Other coupons had varying amounts of deposited corrosion products that corresponded with the inhibition efficiency results. Examples are chromium butyrate treated coupon that had a deposition of uniform corrosion products, and calcium gluconate borate treated that had a non-uniform deposition of pitting corrosion products as seen in Fig. 3.

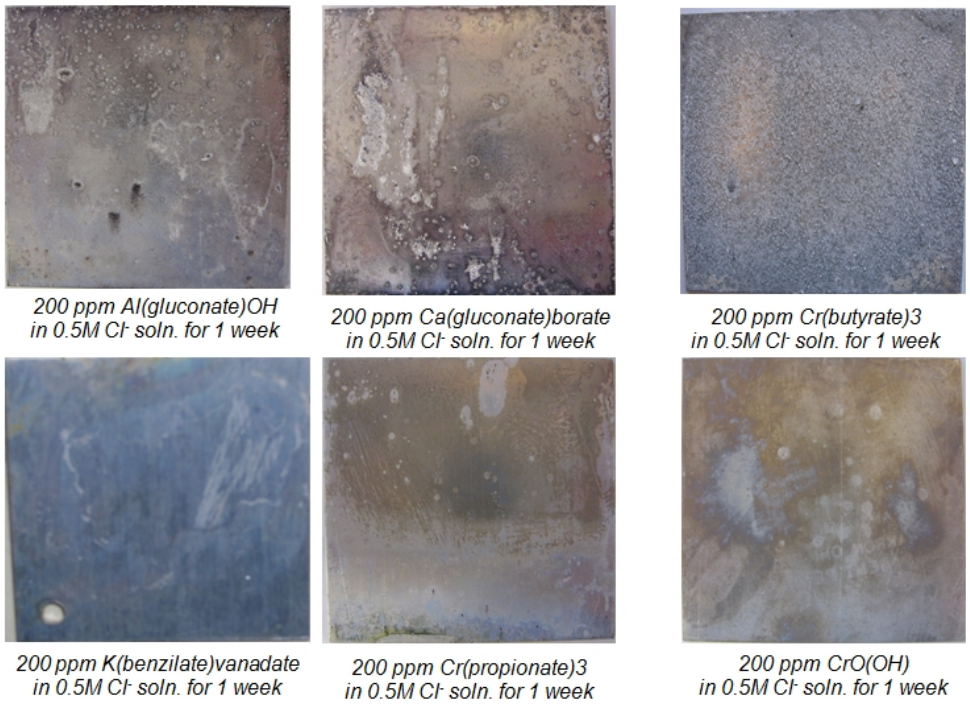

200 ppm Al(gluconate)OH in 0.5M Cl- soln. for 1 week

200 ppm Ca(gluconate)borate in 0.5M Cl- soln. for 1 week

200 ppm Cr(butyrate)3 in 0.5M Cl- soln. for 1 week

200 ppm K(benzilate)vanadate in 0.5M Cl- soln. for 1 week

200 ppm Cr(propionate)3 in 0.5M Cl- soln. for 1 week

200 ppm CrO(OH) in 0.5M Cl- soln. for 1 week

Fig. 3. Images of aluminum 2024 coupons immersed in solutions of various inhibitors

2.2.2 Aluminum 6061 alloy

Coupons treated with inhibitors with high inhibition efficiencies had images of clear surfaces; while ones with very little inhibition efficiencies had deposition of corrosion products on them mostly around pits indicating pitting corrosion. Several such examples are shown in Figs. 4, 5, and 6.

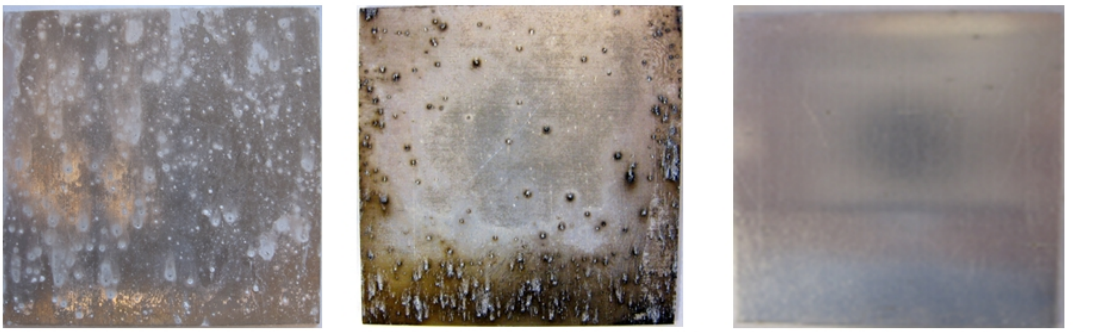

Al 6061 alloy control in 0.5M Cl- soln. for 1 week

200 ppm K (benzilate) molybdate in 0.5 M Cl- soln. for 1 week

200 ppm Zn (gluconate) vanadate in 0.5M Cl- soln. for 1 week

Fig. 4. Images of Control Coupon and Coupons Immersed in Solutions of Metal Oxyanion Esters; respectively

The only exception to the direct relation between inhibition efficiencies and images of clear substrate surfaces was the molybdenum ester treated coupons, which had non-uniform deposition of molybdenum oxides on the surface along with corrosion products around a few pits despite the fact that inhibition efficiencies were close to 100% as revealed in the images in Fig. 5.

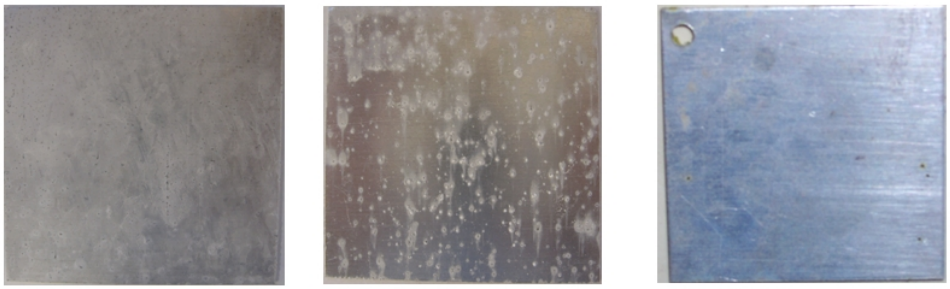

200 ppm Al(gluconate)OH in 0.5M Cl- soln. for 1 week

200 ppm Ca (gluconate)borate in 0.5M Cl- soln. for 1 week

200 ppm K(benzilate)vanadate in 0.5M Cl- soln. for 1 week

Fig. 5. Images of aluminum 6061 coupons immersed in solutions of various inhibitors

200 ppm $Cr(butyrate)_3$ in 0.5M Cl^- soln. for 1 week

200 ppm $Cr(propionate)_3$ in 0.5M Cl^- soln. for 1 week

200 ppm CrO(OH) in 0.5M Cl^- soln. for 1 week

Fig. 6. Images of aluminum 6061 coupons immersed in solutions of various inhibitors

2.2.3 Aluminum 7075 alloy

Among the tested chromium(III) carboxylates for Al 7075 corrosion, chromium butyrate failed to inhibit corrosion, while chromium propionate was more efficient and chromium acetate was the best among the three as shown in Fig. 7. This observation is in agreement with the fact that chromium butyrate is the least and chromium acetate is the most soluble among the three tested chromium(III) carboxylates. Despite being insoluble, the synthesized CrO(OH) inhibited Al 7075 corrosion very efficiently similar to the results with other Al alloys.

200 ppm $Cr(butyrate)_3$ in 0.5M Cl^- soln. for 1 week

200 ppm $Cr(propionate)_3$ in 0.5M Cl^- soln. for 1 week

200 ppm CrO(OH) in 0.5M Cl^- soln. for 1 week

Fig. 7. Images of coupons immersed in various solutions of trivalent chromium compounds

Potassium benzilate molybdate treated Al 7075 coupon resulted in molybdic oxide deposition starting from the edges similar to the other Al alloys of 2024 and 6061 as it can be seen in Fig. 8. It may be speculated that a film of molybdic oxides is more adherent on the edges rather than to the surfaces; since a thinner layer of corrosion products or aluminum oxide is expected on edges than the substrate surface resulting in a higher percentage of pure Aluminum on the edges, which molybdic oxides seemed to better adhere on.

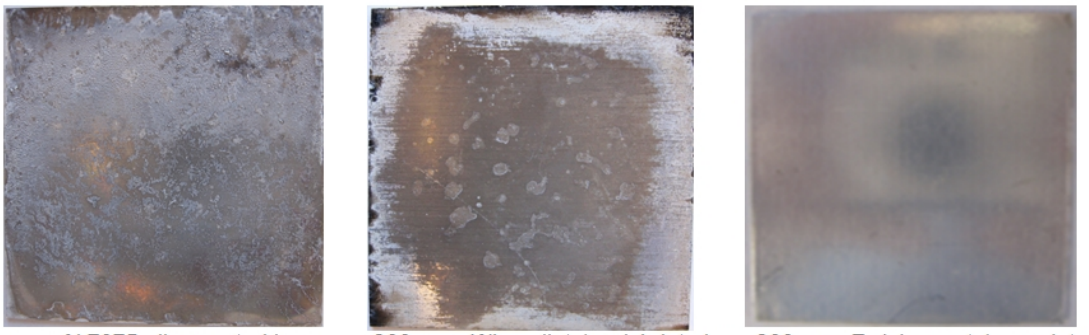

Al 7075 alloy control in 0.5M Cl^- soln. for 1 week

200 ppm K(benzilate)molybdate in 0.5 M Cl^- soln. for 1 week

200 ppm Zn(gluconate)vanadate in 0.5M Cl^- soln. for 1 week

Fig. 8. Images of control coupon and coupons immersed in solutions of metal oxyanion esters; respectively

Coupons treated with calcium gluconate borate revealed virtually no pits, which is in agreement with the inhibition efficiency results of boron esters of hydroxy-acid salts in general as shown in Fig. 9. Boron esters of hydroxy-acid salts inhibited corrosion of Al 7075 alloy considerably higher than the other two alloys. This might have something to do with the composition of Al 7075, which is richer in zinc and magnesium. Borate might react with the magnesium and zinc cations to form insoluble borates and contributing to the passivation layer.

200 ppm Al(gluconate)OH in 0.5M Cl^- soln. for 1 week

200 ppm Ca(gluconate)borate in 0.5M Cl^- soln. for 1 week

200 ppm K(benzilate)vanadate in 0.5M Cl^- soln. for 1 week

Fig. 9. Aluminum 6061 coupons immersed in solutions of various inhibitors

2.3 X-Ray Powder Diffractometer Studies

The X-ray powder diffraction patterns of a blank, untreated Aluminum 2024 alloy and the one treated with K(benzilate)vanadate were identical as shown in Figs. 10 and 11. This correlates with the inhibition efficiency of K(benzilate)vanadate, which was almost perfect even during second immersion period.

The only slight difference between the X-ray diffraction patterns of the two coupons was the very slight strengthening in the peaks due to $Al(OH)_3$ in the X-ray diffraction of the coupon immersed in the salt solution of potassium benzilate vanadate for 7 days.

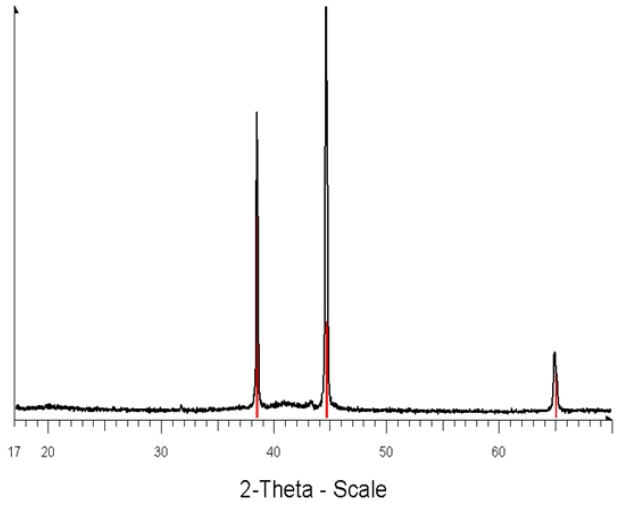

Fig. 10. X-ray diffraction pattern of a blank aluminum 2024 coupon

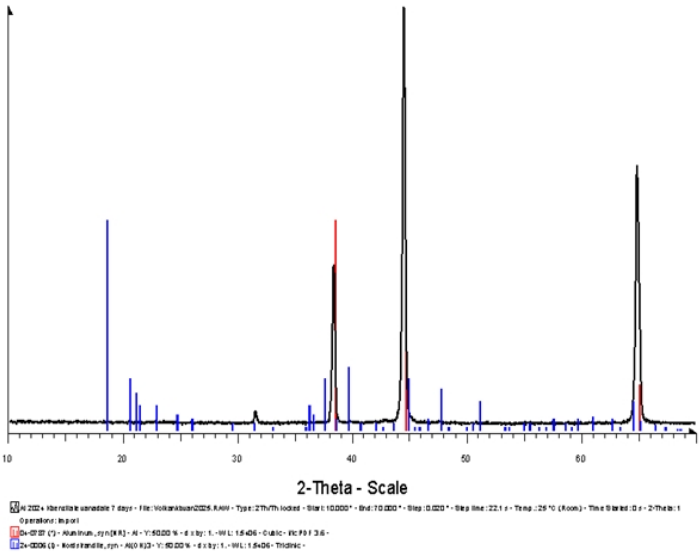

Fig. 11. X-ray diffraction pattern of a 2024 coupon immersed in 200 ppm K(benzilate)vanadate and 0.5M Cl^- solution

2.4 X-Ray Flourescence Studies

X-ray fluorescence (XRF) is a powerful tool to detect tiny amounts of elements on the substrate surfaces. Vanadate esters of hydroxy-acid salts had high inhibition efficiencies with no visually observable conversion coating formation. XRD detected only amorphous phases on the substrate surface but XRF spectroscopy detected vanadium on the substrate surfaces of aluminum alloys as seen in Fig. 12. Vanadium was detected no matter what other constituents were present in the formulation (e.g. zinc gluconate vanadate or potassium benzilate vanadate). The only possible overlap with the ~4 keV vanadium peak

could be due to the L-lines of barium or cesium but even then multiple peaks around the 4 keV range should be present, which was not the case.

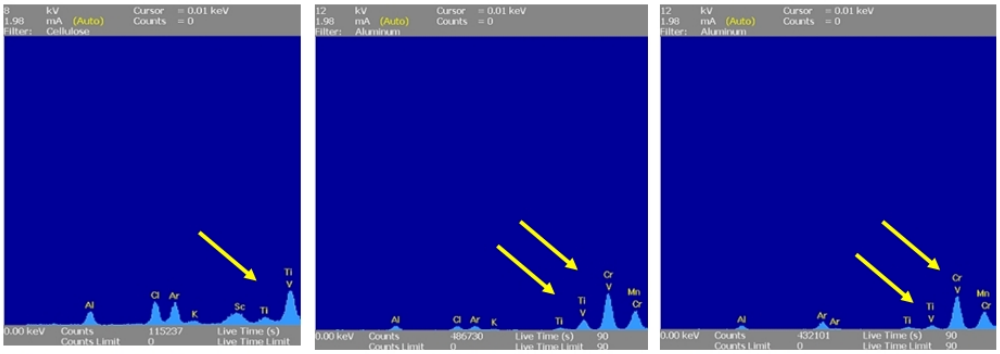

Aluminum 2024 dipped into 200 ppm K(benzilate)vanadate solution

Aluminum 6061 dipped into 200 ppm K(benzilate)vanadate solution

Aluminum 6061 dipped into 200 ppm Zn(gluconate)vanadate solution

Fig. 12. X-ray Flourescence Diagrams of various Aluminum alloycoupons immersed in solutions of vanadium esters of benzilates and gluconates; respectively

2.5 Scanning Electron Microscope Studies

Scanning Electron Micrographs of aluminum alloys immersed in high concentration salt water for one week revealed extensive corrosion taking place on the substrate surfaces as shown in Fig. 13.

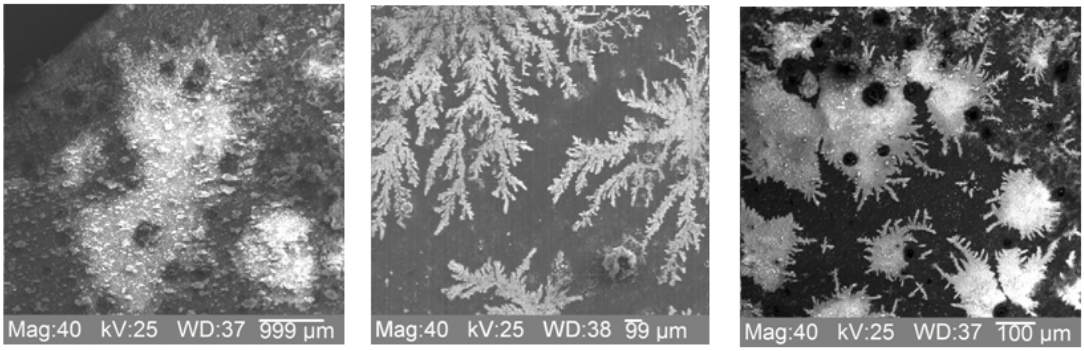

2024 rusted in 0.5 M Cl⁻ water for 7days

6061 in 0.5 M Cl⁻ water for 7days

7075 in 0.5 M Cl⁻ water for 7days

Fig. 13. Scanning electron micrographs of control coupons of various aluminum alloys immersed for 7 Days in 0.5 M chloride solution

Blank and corroded Al substrate samples were examined at lower magnifications for further investigation. Images indicated Al 7075 alloy as more porous than other alloys; while Al 6061 alloy surface was more homogenous than 2024 alloy as shown in Figs. 14, 15 and 16.

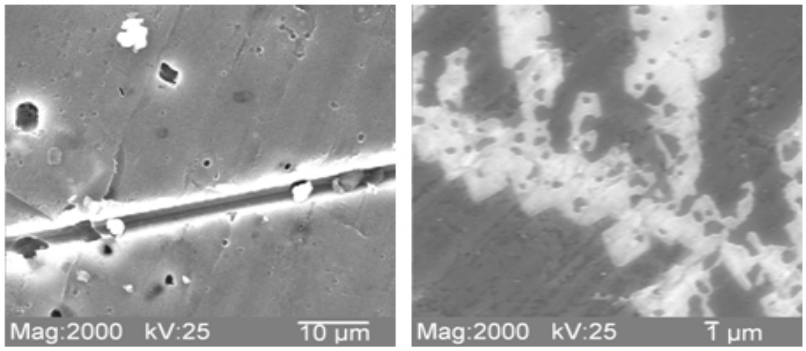

Fig. 14. Scanning electron micrographs of aluminum 2024 alloy coupons

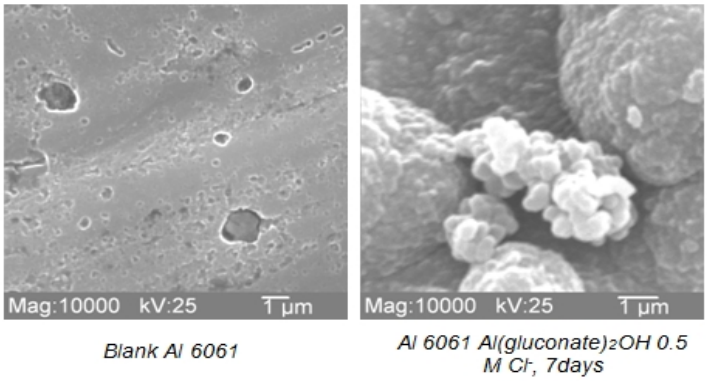

Fig. 15. Scanning electron micrographs of aluminum 6061 alloy coupons

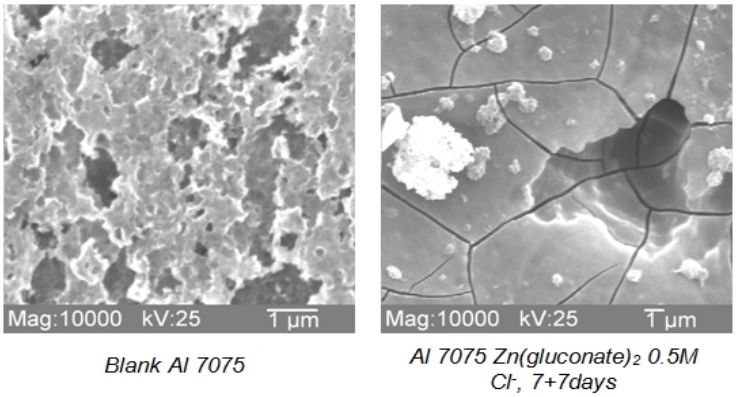

Fig. 16. Scanning electron micrographs of aluminum 7075 alloy coupons

Comparison of the blank substrates with gluconate treated substrates revealed the extent of deposition taking place for the latter as seen in Fig. 17. However, unlike the case for mild

steel, no corrosion protection was observed based on inhibition efficiency results except for the gluconate salts of cations with cathodic inhibitive activity.

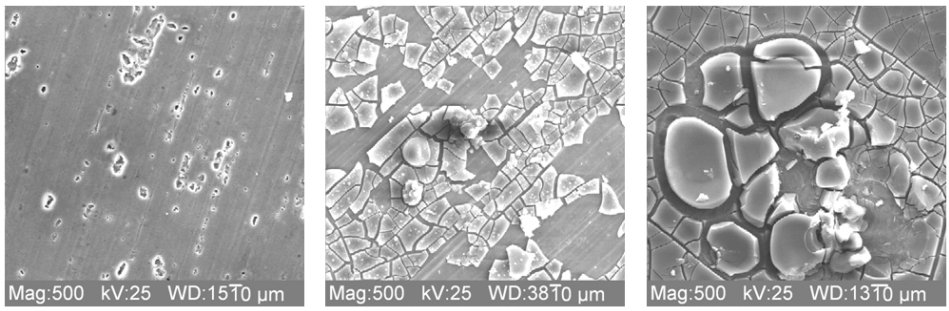

Fig. 17. 500 Times magnified scanning electron micrographs of various aluminum alloys

Consecutive immersions seemed to be destroying the protective coating originated from application of zinc gluconates as it can be seen in Fig. 18.

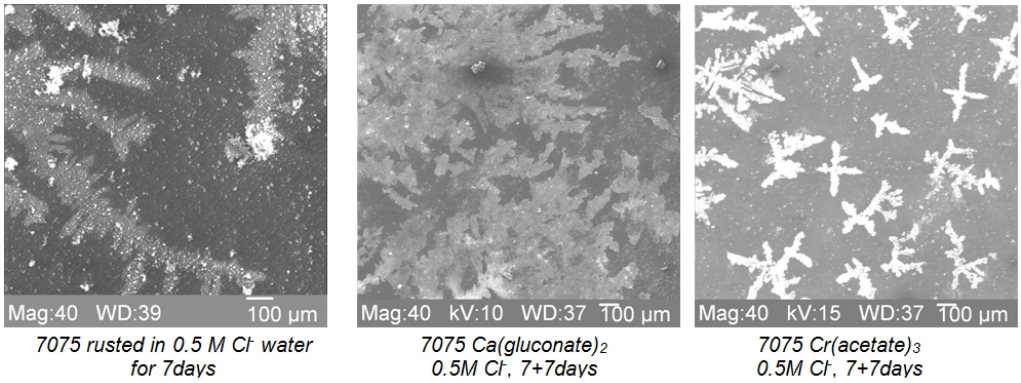

Fig. 18. 40 Times magnified scanning electron micrographs of aluminum 7075 coupons

Scanning electron micrographs of substrates treated with different inhibitors revealed the extent of corrosion during second immersion periods with no inhibitor present in the solution as shown in Fig. 19.

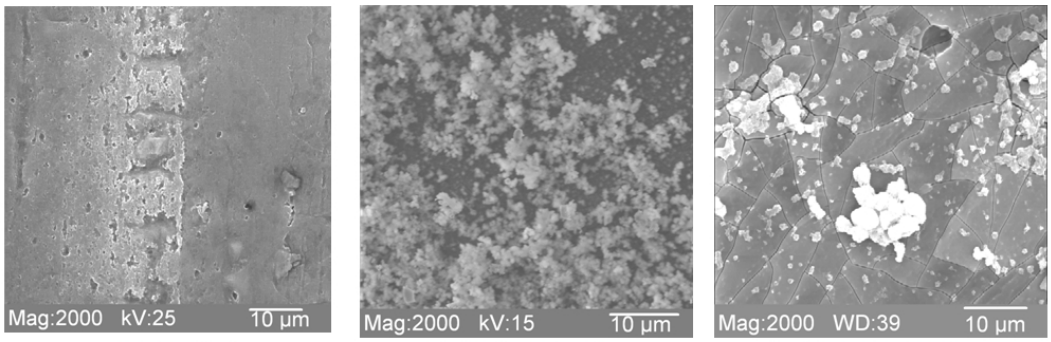

Fig. 19. 2000 times magnified scanning electron micrographs of aluminum 7075 coupons

Immersion of chromium acetate treated Al 7075 coupon for a second period of time revealed abundant corrosion deposits on the substrate surface in agreement with its zero inhibition efficiency during the second immersion period as seen in Fig. 20. Al(gluconate)$_2$OH treated Al 6061 substrates were examined at different magnitudes to investigate the nature of the deposition on the substrate surface.

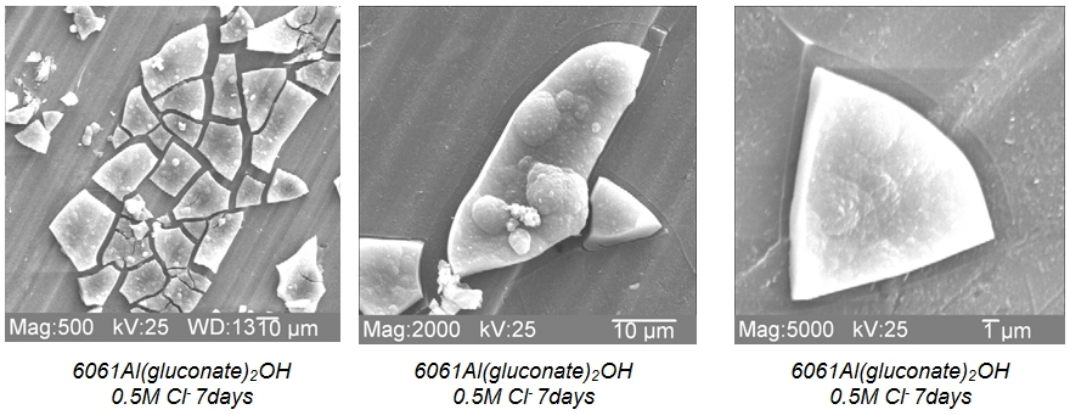

Fig. 20. Scanning electron micrographs of aluminum 6061 coupons immersed in solutions of aluminum gluconate hydroxide

2.6 Infrared Spectra Studies

Infrared spectra studies of inhibitor treated coupons and control coupons have been performed both before and after immersions. Since the substrate surfaces were examined, three types of absorptions were possible; absorptions purely due to structure of the substrate, absorptions purely originated from adsorption of inhibitor compound on the substrate surface, and absorptions due to deposition of compounds such as corrosion products formed by the reactions between the mild steel substrate, the inhibitor compound, and the corrosive chemicals.

The immersion in water is expected to lead to broad bands due to symmetric and asymmetric stretchings of hydroxyl of water centered around 3500 cm^{-1} and due to bending of hydroxyl of water around 1600 cm^{-1} were expected [10-15]. However, the substrates were air dried for several days before taking their spectra to minimize absorptions caused by physically adsorbed water. The difference in absorptions in the 1600 cm^{-1} region of the spectra of control substrates and substrates treated with gluconates, benzilates and other hydroxyl acid salts led to the conclusion that air drying was successful in minimizing the effects of water. Thus, the absorptions around 1600 cm^{-1} region were assigned to carbonyl stretchings in general and specifically to OCO^- stretchings. Other bands in the 1600 cm^{-1} region were assigned to hydroxyl groups of organic compounds rather than hydroxyl of water. IR spectra of different compounds differed depending on the IR active functional groups leading to a categorization based on the IR active constituent.

2.6.1 Gluconate salts

IR spectra of aluminum alloy coupons treated with gluconate salts revealed significant differences than those of IR spectra of mild steel coupons treated with the same gluconate salts. Firstly, three bands were present in the 1400 cm^{-1} – 1600 cm^{-1} range rather than the two bands in the same region for mild steel coupons treated with gluconate salts. Most importantly, these three bands were exact matches of the three bands present in the IR spectra of untreated control coupons.

Therefore, the presence of gluconate moieties on the substrate surfaces of aluminum alloys can be ruled out and the three bands in the 1400 cm^{-1} – 1600 cm^{-1} region can be assigned to the bending of hydroxyl of water of hydrated aluminum oxide, which is a corrosion product, at 1600s cm^{-1} and Al=O bonds at 1400s cm^{-1} [16-17]. Also, the broad band centered at 3450 cm^{-1} is due to symmetric and asymmetric stretchings of hydroxyl of water [18-25]. Loss of the middle band out of these three bands is observed with increasing inhibition efficiency, and the loss of the band in the lower frequency region occurs with even higher inhibition efficiency. The higher frequency band is present at all times suggesting that it is due to the bending vibration of water. Assignment of these three bands to hydroxyl groups and not to carbonyl/carboxyl groups of hydroxy-acids were in agreement with weight-loss test results, which all gluconate salts and other hydroxy-acid salts revealed very low inhibition efficiencies with the exception of zinc gluconates.

Comparison of the IR spectra of the aluminum alloy substrates treated with different amounts of the same inhibitor supported the assignments of the three bands in 1400 cm^{-1} – 1600 cm^{-1} region. One example is comparison of IR spectra of aluminum gluconate hydroxide treated aluminum 2024 alloy coupons as shown in Fig. 21. Comparison of the IR spectra of aluminum gluconate hydroxide powder with those of aluminum 2024 substrates treated with various amounts of aluminum gluconate hydroxide revealed a difference of 20 cm^{-1} between the band due to OCO^- asymmetric stretching and the band due to bending vibration of water hydroxyl, respectively.

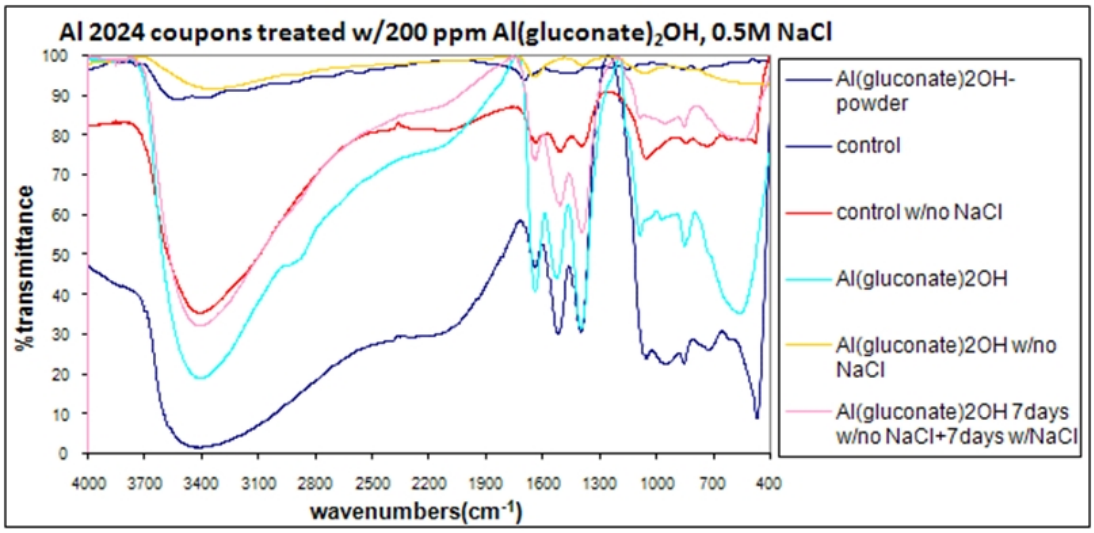

Fig. 21. Combined infrared spectra of aluminum 2024 coupons immersed in aluminum gluconate hydroxide solutions

Notably, the strength of the three main bands in the 1400 cm^{-1} – 1600 cm^{-1} region varied widely based on the concentrations of chloride ions. When no chloride ions were present in the solution only weak absorptions were observed in the IR spectra of aluminum 2024 control coupon in contrast with the IR spectra of aluminum 2024 control coupon immersed in 0.5 M Cl^- solution. Correspondingly, the control coupon with no chloride present in its solution resulted in significantly less weight-loss than the control coupon immersed in 0.5 M Cl^- solution. Changes in absorptions of these bands with increasing corrosion imply the presence of more aluminum hydroxide corrosion products, thus ruling out the assignment of these bands to carbonyl/carboxyl groups once more. The broadening of OH stretching vibrations centered at 3450 cm^{-1} for all tested aluminum alloys substrates was attributed to interactions between the hydroxyl groups with the surface aluminum metal ions [18]. On the other hand, the corrosion products vary with different aluminum alloys and with the use of different inhibitors causing shifting of the bands in the 1400 cm^{-1}-1600 cm^{-1} and 3450 cm^{-1} region as shown in Figs. 22, 23 and 24.

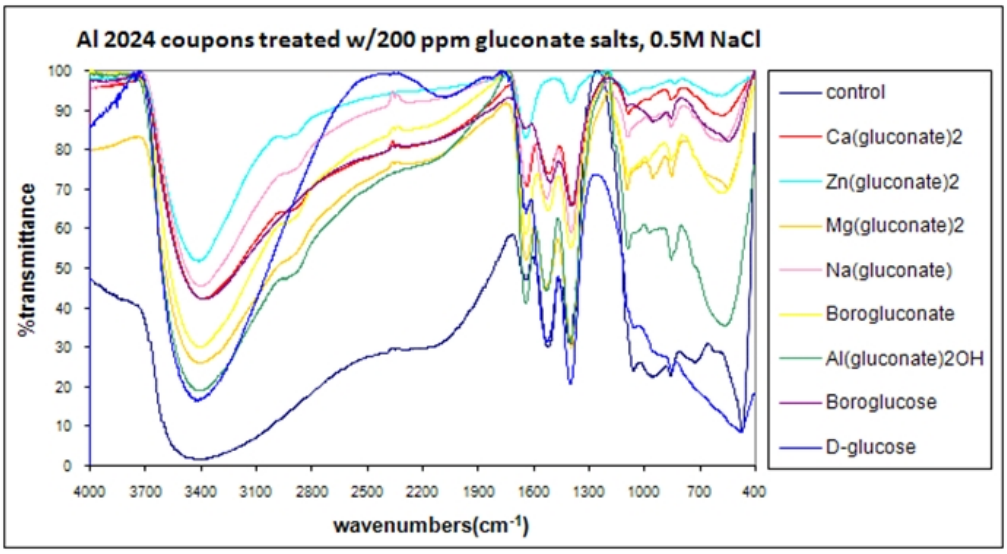

Fig. 22. Combined infrared spectra of aluminum 2024 coupons immersed in solutions of various gluconate and glucose salts

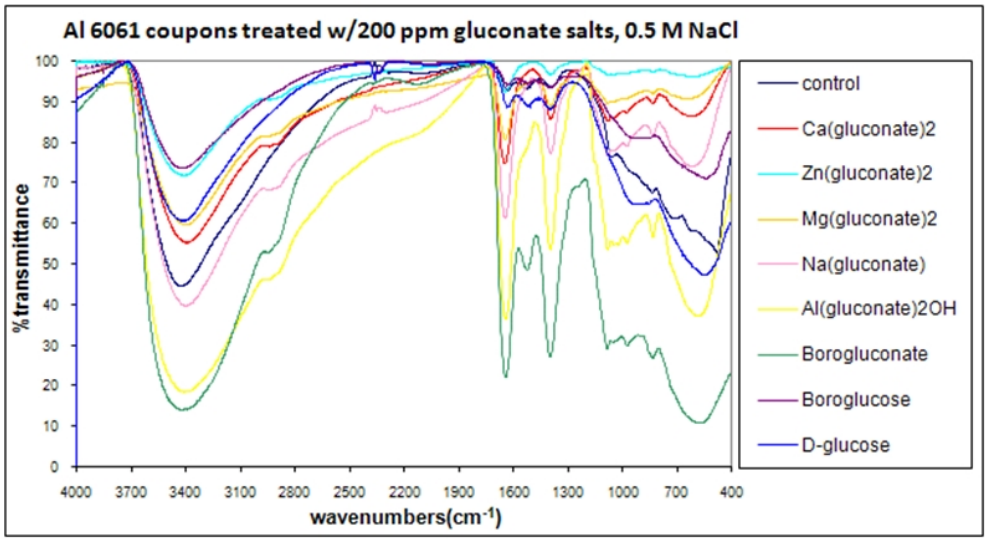

Fig. 23. Combined infrared spectra of aluminum 6061 coupons immersed in solutions of various gluconate and glucose salts

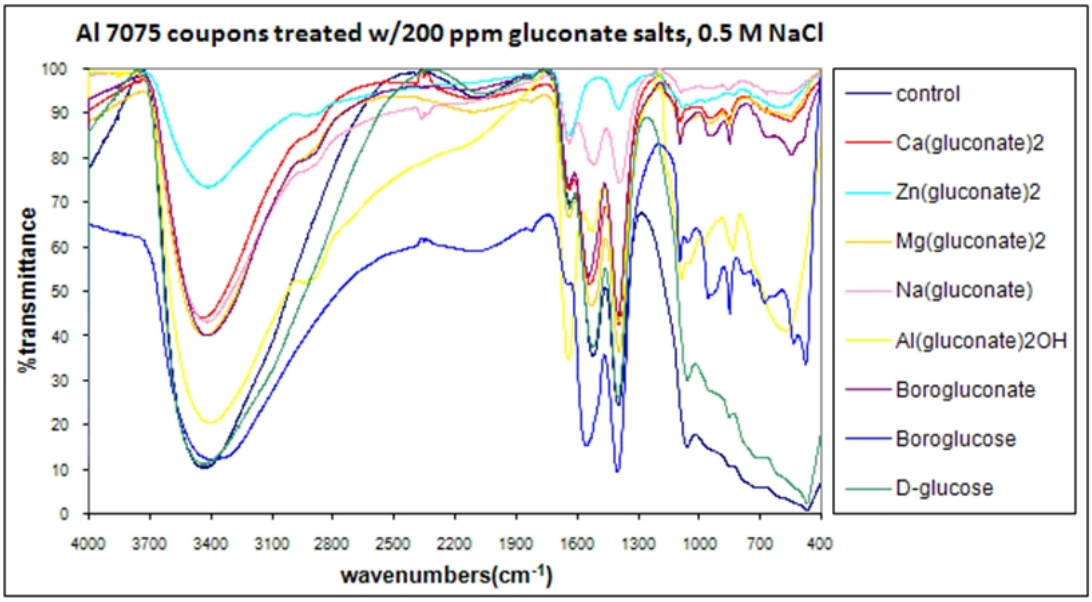

Fig. 24. Combined infrared spectra of aluminum 7075 coupons immersed in solutions of various gluconate and glucose salts

In the low frequency region, bands due to aluminum surface were common for all three tested aluminum alloys albeit with slight differences in frequencies and strengths.

Major peaks in the order of decreasing frequencies, were at 1155 cm^{-1} and 1067 cm^{-1} assigned to OH in-plane bendings of AlOOH, at 1050 cm^{-1} assigned to OH bending vibrations of AlOOH, at 770 cm^{-1} assigned to Al-O stretching vibrations of AlOOH, at 765 cm^{-1} assigned to O^{2-} displacements, at 736 cm^{-1} assigned to OH out of plane bending of AlOOH and at 411 cm^{-1} assigned to displacements of OH^- [26-31].

Notably, the IR spectra of the zinc gluconate treated coupon revealed only two bands in the 1400 cm^{-1} – 1600 cm^{-1} with the middle band missing. Examination of the IR spectra of other coupons treated with inhibitors consisting of zinc cations revealed the same result, indicating that the cause of this effect was due to the zinc ions. Although not confirmed by any spectroscopic technique, the formation of a protective zinc hydroxide film might have hindered the bidentate adsorption of hydroxyl group on the substrate surface. However, the absorption at 1397 cm^{-1}, characteristic of the presence of $Zn(OH)_2$ protective film was not observed [32]. Thus, an alternative explanation, in agreement with middle band missing in the spectra of coupons treated with other highly efficient inhibitors, might be that middle band is due to bending vibration of hydroxyl of aluminum hydroxide that is a corrosion product of Aluminum, which disappears when the corrosion is efficiently inhibited.

2.6.2 Other carboxylic acids and their salts

The infrared spectra of the other tested acids and their salts such as boric acid, aluminum acetate, and aluminum lactate revealed almost entirely the same absorptions as those of the gluconate salts. Even the strengths of the bands due to use of different aluminum alloys matched when both IR spectra of coupons treated with gluconate salts and other

280ydroxyl-acid salts were compared once more leading to the confirmation of the assignments of the bands in the 1400 cm^{-1} – 1600 cm^{-1} region to the bending vibrations of hydroxyl groups.

2.6.3 Molybdenum esters of hydroxy acid salts

The presence of molybdic oxides on aluminum substrate surfaces was apparent from the visual observations. Absorptions due to Mo-O bending vibrational modes normally are observed at 972 cm^{-1} [33], 994 cm^{-1} [34], and 996 cm^{-1} [35] as stated in the literature, however OH bending vibrations of AlOOH also do absorb in the same region. Regardless, a band due to Mo-O bending vibrations present in most of the IR spectra of aluminum coupons exposed to molybdenum esters of hydroxy-acid salts was observed around 990 cm^{-1} as seen in Fig. 25. Notably, bands due to OH bending vibrations above 1000 cm^{-1} were not present in the IR of potassium benzilate molybdate treated coupons suggesting the presence of a barrier film in between water and substrate surface. Bands due to Mo-O bending vibrations also appear in the IR spectra of the coupon immersed for a second period of time, but this time the OH bending vibrations of AlOOH also appear matching the same bands of controls indicating the extent of corrosion taking place despite the layer of molybic oxides.

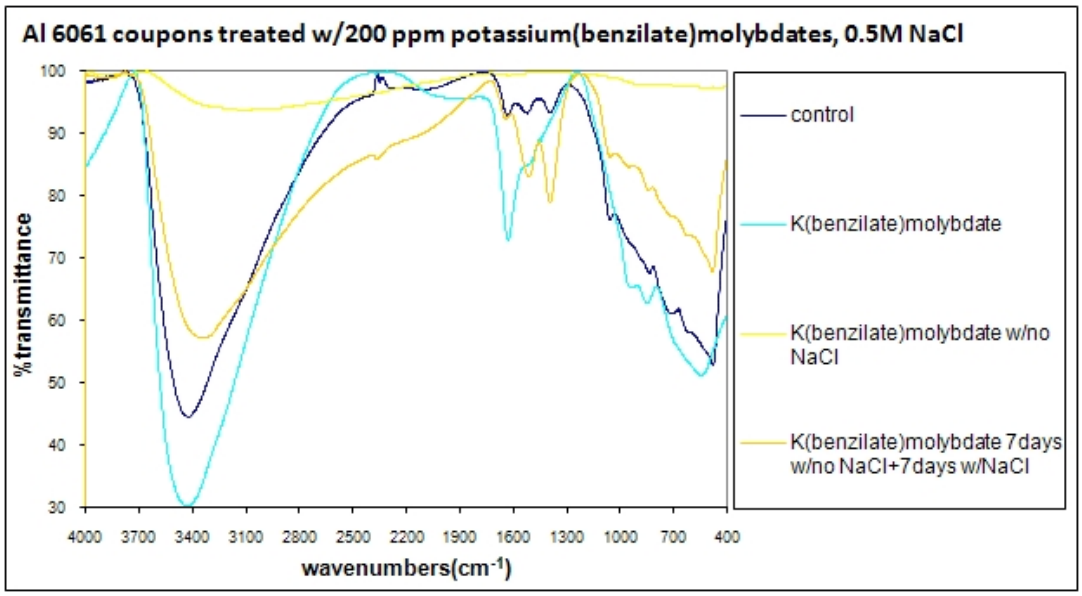

Fig. 25. Combined Infrared Spectra of Aluminum 6061 Coupons Immersed In Potassium Benzilate Molybdate Solutions

Out of the three bands due to bending vibrations of hydroxyl groups, the middle band was found to be missing in the spectra of coupons treated with calcium gluconate molybdates as shown in Fig. 26 and with zinc gluconate molybdates. The highest frequency band among the three bands was also absent in the spectra of coupons treated with potassium benzilate molybdates. Together with weight-loss test results, the absence of bands due to bending vibrations of hydroxyl of water of corrosion product, that is hydrated aluminum oxide, seemed to be an indication for better inhibition efficiency.

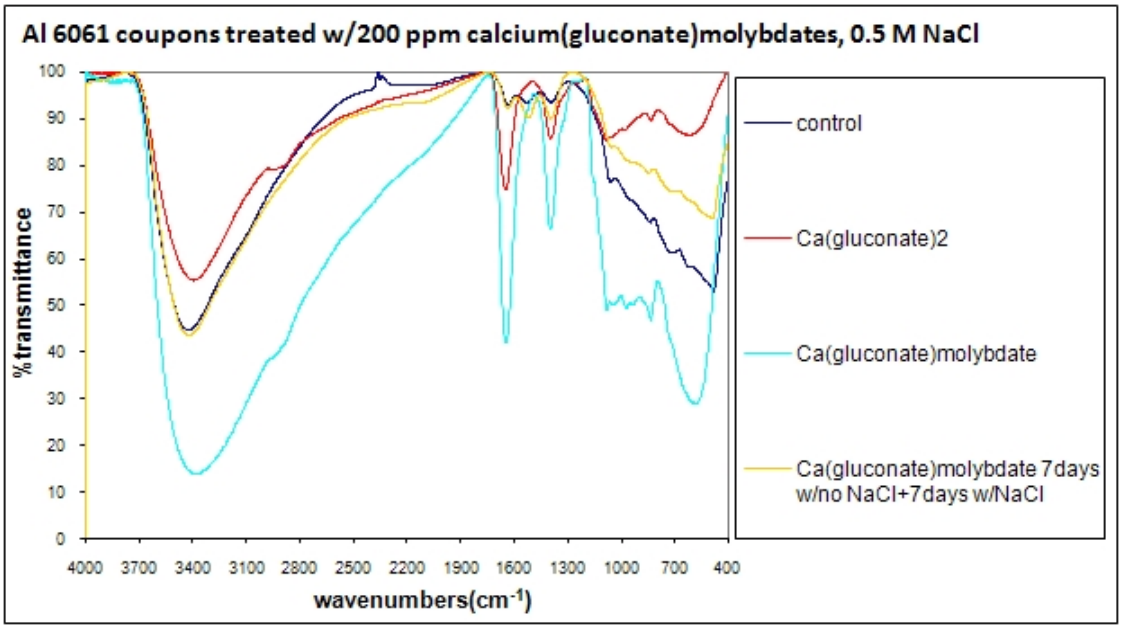

Fig. 26. Combined infrared spectra of aluminum 6061 coupons immersed in calcium gluconate molybdate solutions

2.6.4 Vanadium esters of hydroxy acids

Absorption bands due to presence of vanadium are given in the literature to be between 400 cm^{-1} and 1000 cm^{-1} indexed to various group vibrations of V-O [36-37]. This includes bands at 1019 cm^{-1}, 850 cm^{-1}, and between 400 cm^{-1} to 650 cm^{-1} [38-39]. However, the weak infrared absorptions of the coupons treated with vanadium esters and the presence of many bands due to OH vibrations and stretching of AlOOH in the same region made it impossible to detect the presence of vanadium on the surface. However, along with absence of bands due to vanadium, bands due to corrosion products of aluminum were also absent. IR spectra of coupons treated with vanadium esters for a second period of 7 days seemed similar to the control coupons with missing bands such as the band at 700 cm^{-1} due to stretching vibrations of AlOOH which might be considered as a complimentary evidence for the positive inhibitive efficiencies of vanadium esters during second immersion periods.

2.6.5 Boron esters of hydroxy acids

Spectra of coupons immersed in solutions of boron esters of hydroxy acids almost entirely matched the spectra of the same alloy coupons treated with gluconate and benzilate salts. Thus, almost all IR spectra had three bands due to bending vibrations of hydroxyl of water due to hydrated aluminum oxide in 1600 cm^{-1} region. Coupons treated with zinc salts of borate esters were missing the middle band as in the case of other inhibitors containing zinc cations.

3. DISCUSSION

3.1 Effect of Cationic Constituents

In general the results were opposite to what had been observed in the case of mild steel highlighting the positive effect of metal oxyanions and cationic constituents in the formulation. Gluconate salts and their boron esters were the most efficient inhibitors for mild steel corrosion, while molybdenum and vanadium esters together with formulations consisting of zinc and trivalent chromium cations were most efficient inhibitors for aluminum corrosion. Only zinc cations were found to be an efficient inhibitor for both mild steel and aluminum corrosions.

With sodium gluconate revealing slightly negative inhibition efficiencies, the complexing property of gluconate this time aided the dissolution of protective aluminum oxide coating on the surface. Other gluconate salts such as magnesium gluconate and calcium gluconate inhibited corrosion around 10% unlike sodium gluconate while zinc gluconate effectively inhibited corrosion indicating the sole effect of cationic constituent. Magnesium, calcium, and zinc cations are known for their cathodic inhibitive activity due to forming insoluble hydroxides with zinc cations being the most inhibitive ones. Trivalent chromium was also considered to inhibit corrosion through a similar mechanism in which it forms insoluble chromium hydroxides and oxides.

3.2 Molybdenum and Vanadium Esters of Hydroxy-Acid Salts

Both molybdenum and vanadium esters of 282ydroxyl-acid salts effectively inhibited corrosion of aluminum alloys with potassium benzilate vanadate inhibiting the corrosion very effectively even during a second immersion period, without a supply of inhibitor. There was much evidence for the formation of protective coatings originating from the molybdenum and vanadium esters through surface characterization studies. Digital imaging and infrared spectroscopy provided evidence for deposition of molybdenum on the substrate surfaces in the form of molybdic oxides, while X-ray fluorescence revealed presence of vanadium on the substrate surfaces. Immersion solution studies revealed that formation of trivalent vanadium oxide coatings might not have been due to a redox reaction but rather due to an ion-exchange mechanism between Al^{3+} and V^{3+} cations in the protective aluminum oxide layer leading to the repair and repassivation of the substrate surface resulting in a uniform clear protective coating, while coating of molybdic oxides were formed as a result of a redox reaction between the molybdenum esters of 282ydroxyl-acid salts and the aluminum substrate leading to the formation of a non-uniform albeit protective, rough coating.

4. CONCLUSIONS

Weight-loss tests of the inhibitors for corrosion of aluminum alloys revealed quite different results than those for mild steel. For instance hydroxy-acid salts performed poorly with the exception of zinc gluconate, which was attributed to the cathodic inhibitive activity of zinc cation. Another example was the metal oxyanion esters of hydroxy-acids; molybdate and vanadate esters of hydroxy-acids performed well but borate esters that performed well in the case of mild steel performed poorly for aluminum alloys. Trivalent chromium compounds performed very well in the case of aluminum alloys. Several inhibitors that were not initially tested for mild steel corrosion were also tested for aluminum corrosion; among them were

zinc and trivalent chromium carboxylates, which all performed very well in aqueous solutions provided that the inhibitor is water soluble.

Aluminum gluconate hydroxide was not observed to form a protective coating on aluminum substrates, instead hydroxy-acid esters of molybdates and vanadates seemed to form protective coatings consisting of their lower oxidation state oxides and hydroxides. This was demonstrated by characterization studies via infrared spectra, X-ray fluorescence, and digital imaging. Vanadate esters and benzilate vanadate ester in particular seemed to perform more lasting protective coatings than others.

Based on characterization studies using infrared spectra, scanning electron microscopy, X-ray diffraction, X-ray flourescence spectroscopy, and digital imaging of the substrates conducted in this study as well as on the oxidation-reduction potential, and pH measurements of immersion solutions before and after completion of immersions and on the corrosion inhibiton studies via the weight-loss tests performed by the author in previous studies [40-44]; it was concluded that hydroxy-acid salts, gluconates in particular, slightly damaged the naturally protective aluminum oxide film on the substrate surface by forming complexes with aluminum cations leading to their dissolution. This effect has been minimized when hydroxy-acid salts were complexed with metal oxyanions. Instead, these complexes reacted with aluminum surface to deposit lower oxidation state oxides and hydroxides of the metal oxyanions.

Trivalent chromium compounds performed very well, possibly via a similar mechanism inhibition mechanism of hexavalent chromium forming insoluble oxides and hydroxides of trivalent chromium, only this time there was no hexavalent chromium present in the media.

ACKNOWLEDGEMENTS

Assoc. Prof. Dr. Allen Apblett is acknowledged for the expertise and knowledge he provided me during my PhD education making it possible for me to proceed further in research and science. Also, Ishik University is acknowledged for the financial sponsorship provided for this project.

COMPETING INTERESTS

Author has declared that no competing interests exist.

REFERENCES

1. Cicek V. Trivalent oxychromium compounds replacing carcinogenic hexavalent chromium as corrosion inhibitors for sustainable environment. J of Interdisciplinary Trends In Science And Technology. 2013;388-396.
2. Cicek V, Ozdemir M. Synthesis and characterization of zinc carboxylates as aqueous corrosion inhibitors for mild steel and 2024, 6061, 7075 aluminum alloys. Int J of Chemistry. 2013;5(2):7-11.
3. Cicek V, Ozdemir M. Synthesis and characterization of benzilate esters as aqueous corrosion inhibitors for mild steel and 2024, 6061, 7075 aluminum alloys. Int J of Chemistry. 2013;5(1):26-30.

4. Cicek V, Ozdemir M. Synthesis and characterization of gluconate salts as aqueous corrosion inhibitors for mild steel and 2024, 6061 and 7075 aluminum alloys. J. of Int. Environmental Application and Science. 2012;7(4):802-811.
5. Cicek V, Apblett A. Synthesis and characterization of salts and esters of hydroxy acids as corrosion inhibitors for mild steel and aluminum alloys. J. of Chem. and Chem. Eng. 2011;5:1160-1174.
6. ASTM (American Society for Testing and Materials) Designation, G1–90. Undergone editorial change. Standard Practice for Preparing, Cleaning and Evaluating Corrosion Test Specimen; 1999.
7. ASTM Designation, G31-72. Undergone editorial change, Standard Practice Test for Laboratory Immersion Corrosion Testing of Metals, based upon NACE Standard TM-01-69. Test Method-Laboratory Corrosion Testing of Metals for the Process Industries; 1995.
8. US. Geological Survey, California branch report. Accessed 15 March 2013. Available: http://ca.water.usgs.gov/archive/fact_sheets/b07/up.html.
9. Lahodny-Sarc O. Corrosion in acid mine waters. Yug. Acad. Sc. and Arts. 1982;394:18.
10. Cheng B, Ramamurthy S, McIntyre NS. Characterization of phosphate films on aluminum surfaces. J. of Materials Engineering and Performance. 1997;6(4):405-412.
11. Arnott DR, Hinton BRW, Ryan NE. Cationic Film Forming Inhibitors for the Protection of the AA 7075 Aluminum Alloy Against Corrosion in Aqueous Chloride Solution, Corr. 1989;45(1):12-18.
12. Bishop CV, Foley TJ, Frank JM. Coating solutions of trivalent chromium for coating zinc surfaces. U.S. patent 4,171,231; 1979.
13. Mansfeld F, Wang V, Shih H. Development of “stainless aluminum”. J of Electrochem Soc. 1991;138(12):174-175.
14. Hughes AE, Gorman JD, Paterson PJK. The characterization of Ce-Mo-based conversion coatings on Al-alloys: Part I. Corr Sci. 1996;38(11):1957-1976.
15. Gorman JD, Johnson ST, Johnsto PN, Paterson PJK, Hughes AE. The characterization of Ce-Mo-based conversion coatings on Al-alloys: Part II. Corr Sci. 1996;38(11):1977-1990.
16. Fedrizzi L, Deflorian F, Canteri R, Fedrizzi M, Bonora PL. Progress in the understanding and prevention of corrosion, Proceedings, Barcelona, Spain. 1993(1):131-138.
17. Romans, HB.U.S. Patent. No. 3272665;1966.
18. Miljevic, NR, Katanic-Popovic JD, Matic MD. J Serb Chem Soc. 1988;53:433–437.
19. Dorsey GA. The characterization of anodic aluminas i: composition of films from acidic anodizing electrolytes. J Electrochem Soc. 1966;113:169–172.
20. Rochester, CH, Topham SA. Infrared study of surface hydroxyl groups on haematite, Chem Soc Faraday Trans. 1979;1(75):1073–1088.
21. Walrafen GE, Water A. Water: A Comprehensive Treatise, editor Franks F. Plenum Press, New York. 1972(1):151.
22. Draegert DA, Stone NWB, Curnutte B, Williams D. Far-infrared spectrum of liquid water, J of Opt Soc Am. 1966;56:64.
23. Hasted JB, Husain SK, Frescura FAM, Birch JR. Temperature dependence of the low- and high-frequency raman scattering from liquid water. Chem Phys Lett. 1985;118: 622.
24. Madden PA, Impey RW. Chem Phys Lett. 1986;123:502.
25. Bansil R, Berger T, Toukan K, Ricci MA, Chen SH. A molecular dynamics study of the OH-stretching vibrational spectrum of liquid water. Chem Phys Lett. 1986;132:165.

26. Guillot B. A molecular dynamics study of the far infrared spectrum of liquid water. J of Chem Phys. 1991;95:1543.
27. Corongiu G. Molecular dynamics simulation for liquid water using a polarizable and flexible potential. Int J of Quant Chem. 1992;42:1209.
28. Lewis DG, Farmer VC. Infrared absorption of surface hydroxyl groups and lattice vibrations in lepidocrocite (γ-FeOOH) and boehmite (γ-AlOOH). Clay Minerals. 1986;21:93-100.
29. Parfitt RL, Russell JD, Farmerr VC. Confirmation of the surface structures of goethite (α-FeOOH) and phosphate goethite by infrared spectroscopy. J of Chem Soc. Faraday Trans. 1976;1(72):1082-1087.
30. Parfitt RL, Russell JD. Adsorption on hydrous oxides iv: mechanism of adsorption on various ions on goethite, J of Soil Sci. 1977;28:297-305.
31. Taylor RM. Influence of chloride on the formation of iron oxides from Fe(II) chloride: effect of chloride on the formation of lepidocrocite and crystallinity. Clays Clay Miner. 1984;32:175-180.
32. Misawa T, Kyuno T, Suetaka W, Shimodaira S. The mechanism of atmospheric rusting and the effect of Cu and P on the rust formation of low alloy steels. Corrosion Science. 1971;11:35-48.
33. Misawa T, Asami K, Hashimoto K, Shimodaira S. The mechanism of atmospheric rusting and the protective amorphous rust on low alloy steel. Corrosion Science. 1974; 14:279-289.
34. Rajendran S, Joany RM, Palaniswamy N. An encounter with microheterogeneous systems as corrosion inhibitors. Corrosion Reviews. 2002;20(3):231-252.
35. Irons TV, Stafford FE. J of Am Chem Soc. 1966;88:4819.
36. Ward BG, Stafford FE. Inorg Chem. 1968;7:2569.
37. Barraclough CG, Kew DJ. Aust J of Chem. 1966;19:741.
38. Chen W, Peng J, Mai L, Zhu Q, Xu Q. Synthesis of vanadium oxide nanotubes from V_2O_5 sols. Materials Letters. 2004;58:2277–2278.
39. Wilhartitz P, Dreer S, Ramminger P. Can oxygen stabilize chromium nitride? Characterization of high temperature cycled chromium oxynitride, Thin Solid Films. 2004;293:447–448.
40. Cicek V, Ozdemir M. Aqueous corrosion inhibition studies of aluminum 2024, 6061, and 7075 alloys by oxyanion esters of α-hydroxy acids and their salts, International J of Applied and Natural Sciences. 2013;2(2):9-16.
41. Cicek V, Ozdemir M. Characterization Studies of Aqueous Immersion Solutions of Novel Environmentally Friendly Organometallic Corrosion Inhibitors Used To Cure Aluminum 2024, 6061, and 7075 Alloys Substrates In Corrosive Media, International J. of General Engineering and Technology (IJGET). 2013;2(2):1-16.
42. Cicek V, Ozdemir M. Characterization studies of aqueous immersion solutions of novel environmentally friendly organometallic corrosion inhibitors used to cure mild steel substrates in corrosive media Int J of Engineering Research and Applications. 2013;3(1):1455-1461.
43. Ozdemir D, Cicek V. Aqueous corrosion inhibition studies of mild steel alloy by oxyanion esters of α-hydroxy acids and their salts Int J of Engineering Research and Applications. 2013;3(1):969-985.

44. Cicek V, Ozdemir D. Characterization studies of mild steel alloy substrate surfaces treated by oxyanion esters of α-hydroxy acids and their salts. International Journal of Chemical Science and Technology. 2012;2(3):244-260.

Peer-review history:
The peer review history for this paper can be accessed here:
http://www.sciencedomain.org/review-history.php?iid=230&id=16&aid=1422